ACS Macro Letters

Letter

pubs.acs.org/macroletters

Impact of Interaction Strength and Surface Heterogeneity on the Dynamics of Adsorbed Polymers

Guido Raos* and Julien Idé†

Dipartimento di Chimica, Materiali e Ingegneria Chimica "G. Natta", Politecnico di Milano, via L. Mancinelli 7, 20131 Milano, Italy

Supporting Information

ABSTRACT: We present molecular dynamics simulations of bead-and-spring polymer chains on chemically heterogeneous, energetically disordered surfaces at near-monolayer coverages. The surfaces consist of random mixtures of weakly (W) and strongly (S) attractive sites. We explore systematically the effect of surface composition on the diffusive dynamics of the chains. The polymer diffusion coefficients have a near-Arrhenius temperature dependence, with activation energies which have a nonmonotonic dependence on the fraction of S sites. In other words, we see a nonmonotonic dependence of the interfacial polymer dynamics on its affinity with the surface, when the latter involves some heterogeneity. The maximum activation energy belongs to the surface containing 75% S and 25% W sites, which combines near-maximum average polymer−surface interactions with near-maximum spread or disorder in these interactions. Our results have interesting implications for polymer adhesion and friction and structure−property relationships in polymer nanocomposites.

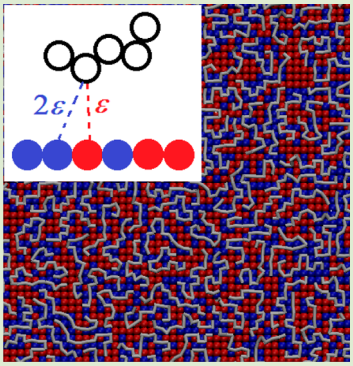

In the closing remarks of a recent review article, Kumar et al.[1] have identified some priority areas for research on polymer nanocomposites. The first topic on their list is the study of the relationship between miscibility, mechanical reinforcement, and polymer glass transition. These are indeed interrelated, as surface functionalizations of the nanoparticles which enhance their compatibility with the polymer matrix often produce a substantial increase of its elastic modulus and fracture toughness[2,3] and, at the same time, a sizable (usually upward) shift of the glass transition, either of the nanocomposite as a whole or of a fraction of material within a few nanometers from the nanoparticles' surface (in the context of filled elastomers, this is the so-called bound rubber or glassy shell[4−6]). Similar effects have also been observed in very thin polymer films on different substrates.[7−9] Nonetheless, the same authors[1] pointed out that these correlations are not universal, and there can be situations where an increase in polymer−particle compatibility is accompanied by a downward shift of the glass transition temperature, or vice versa.[10] The aim of this letter is to present the results of molecular dynamics (MD) simulations on a simple model system, which point to surface heterogeneity as a key feature which might explain these and other, apparently contradictory, observations.

Molecular simulation methods have been applied, among other many things, to study the behavior of supercooled polymers under confinement,[11] polymer nanocomposites,[3,12] polymer−nanoparticle self-assembly,[13] rubber reinforcement,[12,14] and the recognition (through a selective, first-order adsorption transition) between patterned surfaces and copolymers with specified sequences.[15−17] To quote a few more specific examples, we mention some early MD[18] and Monte Carlo[19] simulations demonstrating a dramatic slowdown of the polymer dynamics and the formation of a mechanically hard shell around attractive nanoparticles. Similar effects were seen also in simulations of polymers confined between planar surfaces,[20] which actually showed significant differences between the behavior on an ideally smooth surface and one with small atomic-scale corrugations. We also mention our own mesoscale simulations,[21] providing a direct demonstration of the effect of slowed-down interfacial dynamics (modeled phenomenologically by bistable polymer−filler bonds) on the nonlinear dynamical-mechanical response of particle-filled rubbers (the so-called Payne effect[2,4]). The mechanical deformation and rupture of the glassy polymer bridges between two closely spaced surfaces has also been investigated by nonequilibrium MD simulations.[22]

The simulations mentioned in the previous paragraph assumed relatively smooth, chemically homogeneous surfaces or nanoparticles. Several aspects of the associated phenomena, especially equilibrium ones (e.g., polymer absorption, conformation, and density profiles), have also been thoroughly investigated by a variety of theoretical approaches.[23,24] The situation becomes much richer and challenging, also from a theoretical and computational point of view, once we introduce some heterogeneity or randomness in the surface, the polymer, or both.[15−17,25,26] Here we are specifically interested in the effect of surface heterogeneity on the diffusion and conformational relaxation of adsorbed homopolymer chains. This problem has been studied theoretically by Vilgis and coworkers,[27,28] who described a localization transition of the chains at a critical value of a certain "disorder parameter". The

Received: April 15, 2014
Accepted: July 8, 2014
Published: July 11, 2014

   dx.doi.org/10.1021/mz500233c | ACS Macro Lett. 2014, 3, 721−726

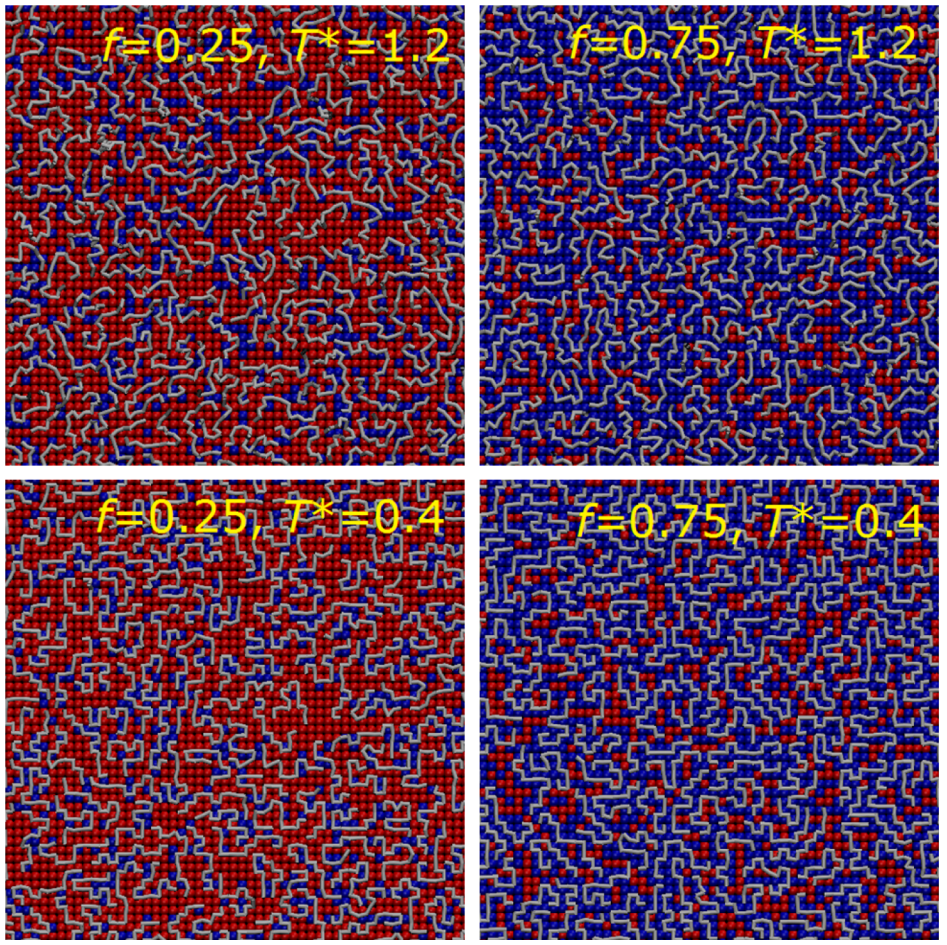

Figure 1. Close-up views of the polymer chains (white strings) on two surfaces with different compositions (f = 0.25 or 0.75) at two different temperatures (T^* = 1.2 and 0.4). The surface's W atoms are red, and the S atoms are blue. These images were produced with the VMD program.[42]

polymer dynamics in this localized state is also characterized by an incomplete (i.e., nonergodic), nonexponential relaxation of the chains' conformation, as described by its Rouse normal modes.[29] There are some strong analogies between this disorder-induced trapping of the polymer chains and the conventional glass transition in supercooled liquids.[30] Roughly speaking, this effect can be expected to be "on top" of the density-induced vitrification, which can occur also in a polymer melt next to a perfectly smooth, attractive surface.[31] Substantial differences in single-chain (or single-particle) diffusive dynamics on clean, ordered surfaces and heterogeneous ones have been seen also experimentally, by atomic force microscopy and fluorescence techniques.[32−35]

We have simulated a series of model systems consisting of several flexible polymer chains, deposited on topographically homogeneous but chemically heterogeneous, energetically disordered surfaces (see Figure 1). Here we only provide a concise description of our approach, as further details can be found in an earlier publication.[36] The polymers are made up of N = 16 "P" beads connected by harmonic springs. The surfaces are perfectly rigid, and they consist of a single layer of atoms arranged on a square planar lattice, at z = 0.0. These atoms can be of two types, henceforth denoted as "W" for weakly and "S" for strongly interacting. Surfaces with different compositions were generated by randomly assigning the type to the surface atoms, with probability f for the S atoms and $1 - f$ for the W ones. Specifically, we ran simulations on surfaces with f = 0.00, 0.12, 0.25, 0.50, 0.75, 0.88, and 1.00. In our model, all nonbonded interactions are described by truncated and shifted Lennard-Jones (LJ) potentials.[37,38] All atoms (P, W, and S) have the same mass m = 1 and hard-core diameter σ = 1 (in reduced LJ units[37,38]). The LJ well depths are as follows (the subscripts denote the involved atom pair): $\varepsilon_{PP} = \varepsilon_{WW} = \varepsilon_{SS} = \varepsilon_{PW} = \varepsilon_{WS} = 1$, while $\varepsilon_{PS} = 2$. Most LJ interactions are truncated at a cutoff distance of 2.5, except for the PP interactions which are truncated at $2^{1/6} \approx 1.122$ to produce a purely repulsive potential. With this choice, at low surface coverages the chains adopt two-dimensional self-avoiding walk conformations whereby their average end-to-end distance and radius of gyration scale as $N^{3/4}$.[36,39] Periodic boundary conditions were adopted in the directions parallel to the surface (x and y). A constant force of −0.1 (in LJ units) was applied to all the P beads along the orthogonal direction, gently pressing them against the underlying surface to prevent any chain detachment (a possibility which we decided to avoid, to simplify the analysis of the MD trajectories). For each system, MD simulations have been conducted at reduced temperatures $T^* = k_B T/\varepsilon_{PP}$ = 1.20, 1.10, 1.00, 0.90, 0.80, 0.70, 0.60, 0.55, 0.50, 0.45, and 0.40. The MD equations of motions were integrated with a time step Δt = 0.01 (again, in reduced LJ units), and the MD production runs typically lasted 10^7 time steps. The simulations were carried out with the COGNAC code.[40]

In our previous paper,[36] we studied the polymers' statistical and dynamical properties (including their response to a pulling

dx.doi.org/10.1021/mz500233c | ACS Macro Lett. 2014, 3, 721−726

force) as a function of chain length (from N = 16 to 256). Those simulations were conducted at very low coverages, on a single disordered surface with f = 0.06. Here, with 450 chains of length N = 16 on surfaces consisting of 100 × 100 atoms, we have a fairly dense, near-monolayer coverage (see again Figure 1; note that these images show only a portion of the systems). These simulation conditions allow us to collect good statistics on the polymer dynamics, without having to deal with the complications of discriminating the behavior of chains or segments at different distances from the surfaces, which would arise in simulations of thicker films or confined polymer melts.[11]

The energetic disorder of a surface can be quantified by the histogram of the interaction energies between a single polymer bead and the surface itself. Qualitatively similar histograms can be obtained experimentally by gas adsorption studies, and they have been shown to be useful for characterizing the reinforcing ability of different fillers.[41] One such histogram is given in the top panel of Figure 2, while the remaining ones are in the

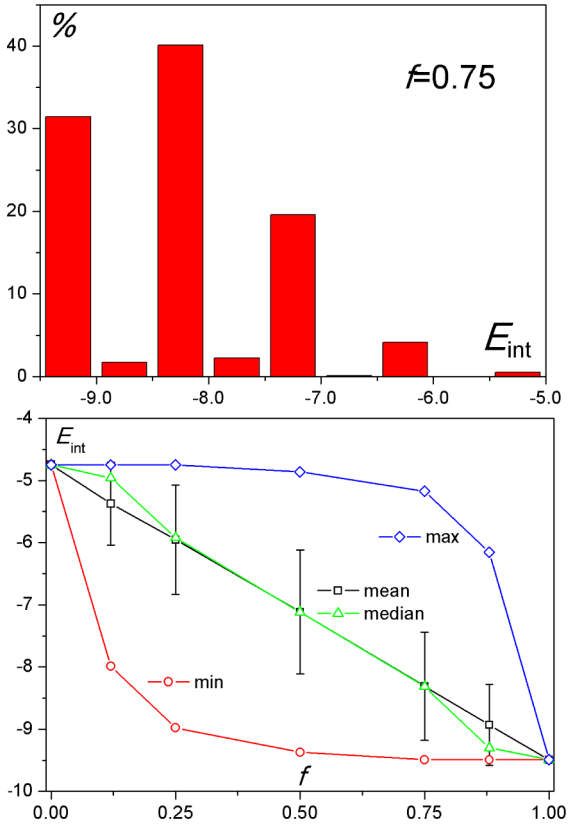

Figure 2. Representative histogram of the interaction energies between a polymer bead and a heterogeneous surface with f = 0.75 (top) and plot summarizing the interaction statistics for all the surfaces (bottom). The vertical bars indicate one standard deviation of the interaction energies.

Supporting Information (SI). It has been constructed by scanning the surface with a P-type LJ bead at a height z = 0.8717, placing it above the centers of the squares formed by four neighboring sites.[36] It reveals a broad and somewhat asymmetric distribution of energies, corresponding to different adsorption environments. The lower panel of Figure 2 summarizes the results for all the surfaces by giving the mean, the median, the standard deviation, the minimum, and the maximum values of these distributions. As expected, the average interaction energy depends linearly on the surface composition. The width of the distribution is maximal at f = 0.50, but it is still quite large for f = 0.25 and 0.75. The distributions are narrower but markedly asymmetric for f = 0.12 and 0.88, as revealed by the difference between the mean and the median. In general, it would be interesting to characterize also the spatial correlation of this energetic disorder, i.e., the correlations in the bead−surface interaction energies at neighboring sites. In the present model, however, these correlations are very short-ranged (at most of the order of the nonbonded cutoff distance of 2.5) as the types of surface atoms (W or S) are assigned in a completely random fashion. Instead, these correlations would be much more important in the case of "patchy" surfaces.

As a prelude to the characterization of the chains' dynamical properties, we have computed the polymer segment density in the direction orthogonal to the surface and the distributions of their end-to-end distances. Several plots are given in the SI. These demonstrate that the chains are strongly adsorbed on the surface, except for the highest temperatures where they can make appreciable excursions away from it up to a couple monomer diameters. The average (root-mean-square) end-to-end distances are always in a fairly narrow range between 5.75 and 5.93. Thus, for all systems and temperatures, the chains adopt an essentially two-dimensional random coil conformation, as they neither desorb nor crystallize on the surfaces.

The chain diffusion coefficients D can be extracted by fitting the time dependence of the mean-square displacements (MSDs) of their centers of mass[36−38]

$$\langle [R_{CM}(t + t_0) - R_{CM}(t_0)]^2 \rangle = 4Dt + b \quad (1)$$

As discussed in the SI, which contains also some representative plots of the MSDs, inclusion of a nonzero intercept b in the fits minimizes the effect of short-time subdiffusive behavior, which can be significant at $T^* < 0.50$ for $f \geq 0.50$. The resulting diffusion coefficients are given in Table 1 and plotted in the upper panel of Figure 3, showing that their temperature dependence roughly follows the Arrhenius behavior

$$\ln(D) = \ln(D_0) - E_a/T^* \quad (2)$$

The resulting activation energies are plotted in the lower panel of Figure 3, showing that they tend to increase with the f fraction of S atoms, but above all, they are maximal when f = 0.75. This nonmonotonic dependence of the activation energy is the central result of this paper, as it illustrates a situation where the system with the most hindered polymer chain dynamics is not the one with the strongest average interactions. Notice also that, besides having that largest activation energy, the systems with f = 0.75 have also the largest uncertainty on it (dashed lines in the plot). This uncertainty is not so large to invalidate our conclusions, but it is nonetheless interesting as it shows that this system has small but appreciable deviations from the Arrhenius behavior (note that, even in this "bad" case, the adjusted R^2 is 0.994). There is clearly an analogy with the behavior of "fragile" supercooled liquids, whose viscosities follow the Vogel−Fulcher−Tamman law rather than the Arrhenius one.[30]

Analogous conclusions apply to the chains' conformational relaxation, monitored through the autocorrelation functions of the Rouse normal modes [$C_q(t)$, where q = 1,2,3, ... is the mode index].[29,36] The upper panel shows some representative decay curves for the most collective and therefore slowest modes,

dx.doi.org/10.1021/mz500233c | ACS Macro Lett. 2014, 3, 721−726

Table 1. Polymer Diffusion Coefficients for Each Reduced Temperature (T^*) and Surface Composition (f)[a]

T^*/f	0.00	0.12	0.25	0.50	0.75	0.88	1.00
0.40	1.0×10^{-4}	1.9×10^{-5}	4.8×10^{-6}	9.0×10^{-7}	4.3×10^{-7}	3.9×10^{-7}	3.9×10^{-7}
0.45	2.4×10^{-4}	5.8×10^{-5}	1.5×10^{-5}	2.8×10^{-6}	9.9×10^{-7}	9.0×10^{-7}	1.3×10^{-6}
0.50	4.4×10^{-4}	1.4×10^{-4}	4.3×10^{-5}	7.9×10^{-6}	3.2×10^{-6}	3.1×10^{-6}	3.8×10^{-6}
0.55	7.1×10^{-4}	2.9×10^{-4}	1.1×10^{-4}	2.0×10^{-5}	8.4×10^{-6}	7.7×10^{-6}	9.6×10^{-6}
0.60	0.0012	4.7×10^{-4}	1.9×10^{-4}	4.7×10^{-5}	2.2×10^{-5}	2.0×10^{-5}	2.0×10^{-5}
0.70	0.0021	0.0012	6.3×10^{-4}	1.7×10^{-4}	7.6×10^{-5}	6.8×10^{-5}	7.2×10^{-5}
0.80	0.0041	0.0024	0.0012	4.9×10^{-4}	2.4×10^{-4}	2.0×10^{-4}	1.8×10^{-4}
0.90	0.0057	0.0035	0.0024	0.0010	5.1×10^{-4}	4.4×10^{-4}	4.2×10^{-4}
1.00	0.0085	0.0058	0.0041	0.0020	0.0011	8.8×10^{-4}	7.5×10^{-4}
1.10	0.013	0.0085	0.0058	0.0033	0.0018	0.0014	0.0013
1.20	0.016	0.011	0.0087	0.0045	0.0029	0.0022	0.0019
E_a	3.00 ± 0.05	3.78 ± 0.03	4.51 ± 0.04	5.29 ± 0.08	5.52 ± 0.14	5.40 ± 0.12	5.18 ± 0.07

[a]The last row gives the activation energies and their standard errors.

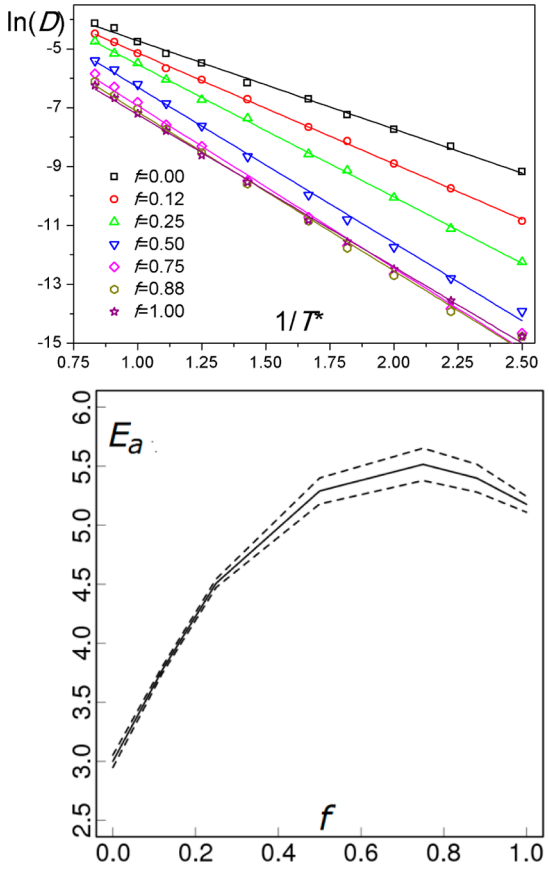

Figure 3. Arrhenius plots of the chain diffusion coefficients (top) and plot illustrating the surface dependence of the activation energies (bottom). The dashed lines indicate the standard errors, as obtained from the least-squares fits of the Arrhenius plots.

plotted in semilog form to highlight a near-exponential decay, as predicted by the Rouse model

$$C_q(t) = \exp\{-t/\tau_p\} \tag{3}$$

where the most collective modes (small p) are expected to decay more slowly[29]

$$\tau_p \sim N^2/p^2 \quad (p \ll N) \tag{4}$$

At high temperatures, these modes do decay as predicted by eq 3. However, conformational relaxation becomes dramatically slower at lower temperatures or higher disorder, to the point that it might be better described by the more general law[27,28]

$$C_q(t) \cong \exp\left\{-\left(\frac{t}{\tau_p}\right)^{\beta}\right\} + r(q) \tag{5}$$

where $0 < \beta < 1$ is a "stretching exponent" and $0 < r(q) < 1$ a "nonergodicity parameter". Looking at the plots for $T^* = 0.4$ and 0.5, a nonexponential relaxation seems indeed quite likely, but for simplicity in the data analysis and their interpretation, even in these cases we have fitted the initial decay of the Rouse correlation functions using eq 3. The resulting relaxation rates (inverse of the relaxation times) also have a near-Arrhenius temperature dependence. The activation energies for the first three normal modes are plotted in the lower part of Figure 4. Their surface dependence closely resembles that for translational diffusion, reaching a maximum for the surface with $f = 0.75$.

Finally, one may speculate about the origin of the observed nonmonotonic variation in the polymer dynamics. Looking back at Figure 2, we see that the surface with $f = 0.75$ combines near-maximum polymer–surface attraction with near-maximum surface heterogeneity (the maxima of these individual properties are clearly at $f = 1.0$ and $f = 0.5$, respectively). At a coarse-grained level, a chain which is already absorbed in a very favorable configuration will have an energetic incentive to diffuse along its own path, so it might be possible to interpret its dynamics in terms of a reptation model.[29,32] However, at the local scale—i.e., the scale which determines the activation energies—diffusion of a strongly absorbed polymer must involve conformational transitions of its segments, jumping from one to another adsorption site (see Figure 5). Sometimes, "unlocking" a particularly favorable situation may require a jump from a strongly to a weakly adsorbing site. These local transitions may involve more energy than those on a strongly interacting but homogeneous surface and therefore will tend to raise the overall activation energy for diffusion of the chains. In fact, it seems quite reasonable that the measured activation energies should depend on the whole distribution of polymer–surface interaction energies and not just on its average value.

To sum up, we have presented some MD simulations on a simple model system, which show that the polymer dynamics next to a solid surface can have a nonmonotonic dependence on their "affinity" (f, in our model). Our main conclusion,

dx.doi.org/10.1021/mz500233c | ACS Macro Lett. 2014, 3, 721–726

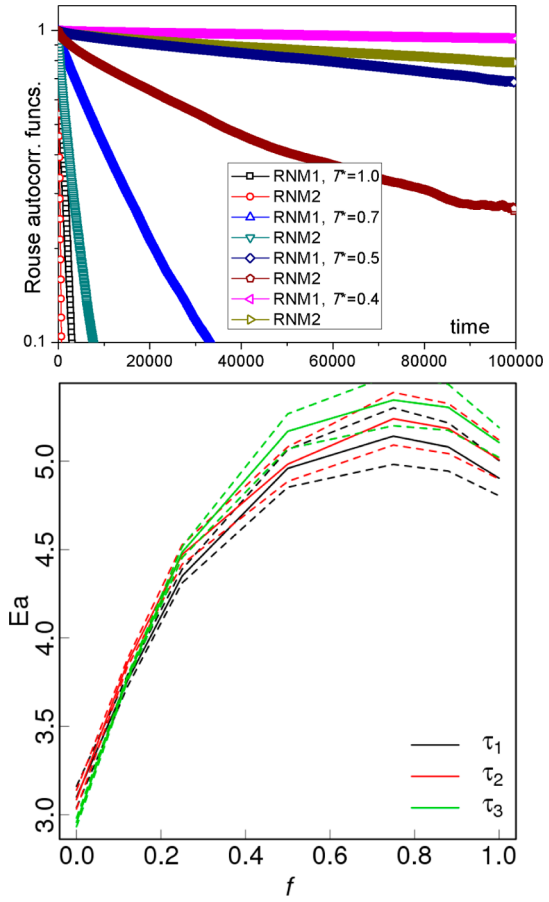

Figure 4. Semilog plots of the autocorrelation functions of the first two Rouse normal modes (RNM1 and RNM2), for the chains on a surface with $f = 0.5$ at selected temperatures (top). Plots illustrating the surface dependence of the activation energies, extracted from Arrhenius fits of the Rouse relaxation times (bottom).

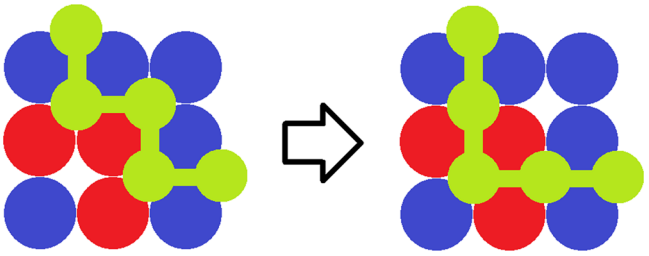

Figure 5. Simplified picture of a conformational transition of a polymer on a heterogeneous surface (S atoms in blue, W atoms in red). One monomer jumps from a more to a less energetically favorable site.

which might be relevant for polymer adhesion and friction on solid surfaces, is that reducing their affinity might actually slow down the polymer relaxation (i.e., increase the activation energy for diffusion), possibly shifting its glass transition temperature upward, when this reduction is achieved through an increase of the surface heterogeneity. We are now planning to investigate composites containing heterogeneous nanoparticles, to check its validity also in situations where there is a bulk polymer (instead of a monolayer) in contact with curved or more irregular surfaces. Hopefully, these studies will contribute to the development of better polymer-based materials, combining more facile processing with improved mechanical properties.

■ ASSOCIATED CONTENT

Supporting Information

Histograms of the interaction energies for all the surfaces, characterization of the static equilibrium properties of the polymer chains (density profiles, end-to-end distances), and further discussion of the chain diffusion coefficients. This material is available free of charge via the Internet at http://pubs.acs.org.

■ AUTHOR INFORMATION

Corresponding Author

*E-mail: guido.raos@polimi.it. Phone: +39-02-2399-3051. Fax: +39-02-2399-3180.

Present Address

†Julien Idé, Laboratory for Chemistry of Novel Materials, University of Mons, Place du Parc 20, BE-7000 Mons, Belgium.

Notes

The authors declare no competing financial interest.

■ ACKNOWLEDGMENTS

This work was supported by the PRIN project on "Nanostructured Polymeric Materials" (ref 2010XLLNM3). Computer time was provided by CINECA and Regione Lombardia through the LISA and ISCRA initiatives (SIPONS and NINAPINT projects).

■ REFERENCES

(1) Kumar, S. K.; Jouault, N.; Benicewicz, B.; Neely, T. *Macromolecules* **2013**, *46*, 3199−3214.
(2) Vilgis, T. A.; Heinrich, G.; Kluppel, M. *Reinforcement of Polymer Nanocomposites: Theory, Experiments and Applications*; Cambridge University Press: Cambridge, 2009.
(3) Jancar, J.; Douglas, J. F.; Starr, F. W.; Kumar, S. K.; Cassagnau, P.; Lesser, A. J.; Sternstein, S. S.; Buehler, M. J. *Polymer* **2010**, *51*, 3321−3343.
(4) Wang, M. J. *Rubber Chem. Technol.* **1998**, *71*, 520−589.
(5) Raos, G. *Macromol. Theory Simul.* **2003**, *12*, 17−23.
(6) Papon, A.; Montes, H.; Lequeux, F.; Oberdisse, J.; Saalwächter, K.; Guy, L. *Soft Matter* **2012**, *8*, 4090−4096.
(7) Fryer, D. S.; Peters, R. D.; Kim, E. J.; Tomaszewski, J. E.; de Pablo, J. J.; Nealey, P. F.; White, C. C.; Wu, W. *Macromolecules* **2001**, *34*, 5627−5634.
(8) Rittigstein, P.; Priestley, R. D.; Broadbelt, L. J.; Torkelson, J. M. *Nat. Mater.* **2007**, *6*, 278−282.
(9) Ediger, M. D.; Forrest, J. A. *Macromolecules* **2014**, *47*, 471−478.
(10) Bansal, A.; Yang, H.; Li, C.; Benicewicz, B. C.; Kumar, S. K.; Schadler, L. S. *J. Polym. Sci., Part B: Polym. Phys.* **2006**, *44*, 2944−2950.
(11) Baschnagel, J.; Varnik, F. *J. Phys.: Condens. Matter* **2005**, *17*, R851−R953.
(12) Allegra, G.; Raos, G.; Vacatello, M. *Prog. Polym. Sci.* **2008**, *33*, 683−731.
(13) Yan, L.-T.; Xie, X.-M. *Prog. Polym. Sci.* **2013**, *38*, 369−405.
(14) Liu, J.; Zhang, L.; Cao, D.; Shen, J.; Gao, Y. *Rubber Chem. Technol.* **2012**, *85*, 450−481.
(15) Muthukumar, M. *J. Chem. Phys.* **1995**, *103*, 4723−4731.
(16) Golumbfskie, A. J.; Pande, V. S.; Chakraborty, A. K. *Proc. Natl. Acad. Sci. U.S.A.* **1999**, *96*, 11707−11712.
(17) Jayaraman, A.; Hall, C. K.; Genzer, J. *Phys. Rev. Lett.* **2005**, *94*, 078103−1/4.
(18) Starr, F. W.; Schrøder, T. B.; Glotzer, S. C. *Macromolecules* **2002**, *35*, 4481−4492.
(19) Papakonstantopoulos, G.; Yoshimoto, K.; Doxastakis, M.; Nealey, P.; de Pablo, J. *Phys. Rev. E* **2005**, *72*, 031801−1/6.
(20) Smith, G. D.; Bedrov, D.; Borodin, O. *Phys. Rev. Lett.* **2003**, *90*, 226103−1/4.

(21) Raos, G.; Casalegno, M. *J. Chem. Phys.* **2011**, *134*, 054902/1−14.
(22) Froltsov, V. A.; Klüppel, M.; Raos, G. *Phys. Rev. E* **2012**, *86*, 041801/1−10.
(23) Yethiraj, A. *Adv. Chem. Phys.* **2002**, *121*, 89−139.
(24) Netz, R. R.; Andelman, D. *Phys. Rep.* **2003**, *380*, 1−95.
(25) Baumgärtner, A.; Muthukumar, M. *Adv. Chem. Phys.* **1996**, *94*, 625−708.
(26) Chakraborty, A. *Phys. Rep.* **2001**, *342*, 1−61.
(27) Migliorini, G.; Rostiashvili, V. G.; Vilgis, T. A. *Eur. Phys. J. B: Condens. Matter* **2003**, *33*, 61−73.
(28) Vilgis, T. A. *Polymer.* **2005**, *46*, 4223−4229.
(29) Doi, M.; Edwards, S. F. *The Theory of Polymer Dynamics*; Oxford University Press: Oxford, 1988.
(30) Berthier, L.; Biroli, G. *Rev. Mod. Phys.* **2011**, *83*, 587−645.
(31) McCoy, J. D.; Curro, J. G. *J. Chem. Phys.* **2002**, *116*, 9154−9157.
(32) Kumaki, J.; Kawauchi, T.; Yashima, E. *Macromolecules* **2006**, *39*, 1209−1215.
(33) Xu, Q.; Feng, L.; Sha, R.; Seeman, N. C.; Chaikin, P. M. *Phys. Rev. Lett.* **2011**, *106*, 228102−1/4.
(34) Wong, J. S. S.; Hong, L.; Bae, S. C.; Granick, S. *Macromolecules* **2011**, *44*, 3073−3076.
(35) Skaug, M. J.; Mabry, J.; Schwartz, D. K. *Phys. Rev. Lett.* **2013**, *110*, 256101−1/5.
(36) Raos, G.; Sluckin, T. J. *Macromol. Theory Simul.* **2013**, *22*, 225−237.
(37) Allen, M. P.; Tildesley, D. J. *Computer Simulation of Liquids*; Clarendon Press: Oxford, 1987.
(38) Frenkel, D.; Smit, B. *Understanding Molecular Simulation*, 2nd ed.; Academic Press: New York, 2002.
(39) Yethiraj, A. *Macromolecules* **2003**, *36*, 5854−5862.
(40) Aoyagi, T.; Sawa, F.; Shoji, T.; Fukunaga, H.; Takimoto, J.; Doi, M. *Comput. Phys. Commun.* **2002**, *145*, 267−279.
(41) Schröder, A.; Klüppel, M.; Schuster, R. H. *Macromol. Mater. Eng.* **2007**, *292*, 885−916.
(42) Humphrey, W.; Dalke, A.; Schulten, K. *J. Mol. Graphics* **1996**, *14*, 33−38.